Microsc. Microanal. 23, 989–1001, 2017
doi:10.1017/S1431927617012363

Microscopy AND Microanalysis

Low Doses of Simvastatin Potentiate the Effect of Sodium Alendronate in Inhibiting Bone Resorption and Restore Microstructural and Mechanical Bone Properties in Glucocorticoid-Induced Osteoporosis

Priscila L. Sequetto,[1,2] Reggiani V. Gonçalves,[3] Aloísio S. Pinto,[4] Maria G. A. Oliveira,[2] Izabel R. S. C. Maldonado,[5] Tânia T. Oliveira,[2] and Rômulo D. Novaes[6,*]

[1]*Department of Pharmaceutical Sciences – Health Area, Universidade Federal de Juiz de Fora, Governador Valadares, 35020-220, MG, Brazil*
[2]*Department of Biochemistry and Molecular Biology, Universidade Federal de Viçosa, Viçosa, 36570-000, MG, Brazil*
[3]*Department of Animal Biology, Universidade Federal de Viçosa, MG, Brazil*
[4]*Department of Veterinary Medicine, Universidade Federal de Viçosa, Viçosa, 36570-000, MG, Brazil*
[5]*Department of General Biology, Universidade Federal de Viçosa, Viçosa, 36570-000, MG, Brazil*
[6]*Institute of Biomedical Sciences, Department Structural Biology, Universidade Federal de Alfenas, Alfenas, 37130-001, MG, Brazil*

Abstract: By using an experimental model of dexamethasone-induced osteoporosis we investigated the effects of different therapeutic schemes combining sodium alendronate (SA) and simvastatin on bone mineral and protein composition, microstructural and mechanical remodeling. Wistar rats were randomized into eight groups: G1: non-osteoporotic; G2: osteoporotic; G3, G4, and G5: osteoporotic + SA (0.2, 0.4, and 0.8 mg/kg, respectively); G6, G7, and G8: osteoporotic + SA (0.2, 0.4, and 0.8 mg/kg, respectively) + simvastatin (0.4, 0.6, and 1 mg/kg, respectively). Osteoporosis was induced by dexamethasone (7 mg/kg, i.m.) once a week for 5 weeks. All treatments were administered for 8 weeks. Dexamethasone increased serum levels of alkaline phosphatase, calcium, phosphorus, and urea, especially in non-treated animals, which showed severe osteoporosis. Dexamethasone also induced bone microstructural fragility and reduced mechanical resistance, which were associated with a marked depletion in mineral mass, collagenous and non-collagenous protein levels in cortical and cancellous bone. Although SA has attenuated osteoporosis severity, the effectiveness of drug therapy was enhanced combining alendronate and simvastatin. The restoration in serum parameters, organic and inorganic bone mass, and mechanical behavior showed a dose-dependent effect that was potentially related to the complementary mechanisms by which each drug acts to induce bone anabolism, accelerating tissue repair.

Key words: bone, glucocorticoid, microanalysis, pathology, scanning electron microscopy

Introduction

Osteoporosis is a metabolic bone disease characterized by low bone mineral density and macro and microstructural deterioration, resulting in increased bone fragility and fracture risk (de Vries et al., 2007; Wheater et al., 2013; Dai et al., 2016). The osteoporosis etiology is complex and multifactorial (Weinstein, 2001; Bonucci & Ballanti, 2014). Osteoporosis can be observed throughout the natural aging process and health factors, such as hormonal disorders, a sedentary lifestyle and immobility, inadequate nutrient intake, metabolic and chronic inflammatory diseases, as well as prolonged use of drugs, can aggravate bone loss and accelerate osteoporosis development (Rosenson et al., 2005; Dimic et al., 2010; Weinstein, 2012).

Glucocorticoids are often used to suppress inflammatory and autoimmune diseases, including those associated with joint and periarticular bone destruction (Manelli & Giustina, 2000; Briot & Roux, 2015). As a serious side effect, long-term treatment with glucocorticoids is associated with morphofunctional disorders in connective tissues, including bone, which may lead to osteopenia, osteoporosis, and increased risk of fractures (Miller et al., 2000; de Vries et al., 2007; Khosla et al., 2012). Glucocorticoid-based chemotherapy is a frequent cause of osteoporosis in humans (Sasaki et al., 2001; Briot & Roux, 2015). These steroidal hormones can directly affect bone by altering osteoclast, osteoblast, and osteocyte number, and by decreasing cell activity or survival (Mclaughlin et al., 2002; Bonucci & Ballanti, 2014; Briot & Roux, 2015). Dexamethasone is a glucocorticoid that is six times more potent than prednisone and has a lifetime of 36–72 h in blood (Shefrin & Goldman, 2009). In osteoblasts, dexamethasone acts by inhibiting cell proliferation and extracellular matrix synthesis (Manelli & Giustina, 2000; Hurson et al., 2007; Weinstein, 2012). There is evidence that dexamethasone increases osteoclast proliferation (Nakashima & Haneji, 2013; Briot & Roux, 2015), and reduces bone formation and turnover in mice (Mclaughlin et al., 2002; Jia et al., 2006). Furthermore, a marked reduction in osteocalcin serum levels and increased bone structural

Received November 19, 2016; accepted June 19, 2017
*Corresponding author. romuonovaes@yahoo.com.br

fragility are also observed in patients undergoing dexamethasone therapy (Sasaki et al., 2001; Oryan et al., 2015).

Bisphosphonates, and more recently statins, have been used in therapeutic protocols to treat bone diseases with different etiologies (Dimic et al., 2010; Rogers et al., 2011; Khosla et al., 2012; Oryan et al., 2015). Due to their efficacy, safety, and remarkable selectivity for bone tissue, bisphosphonates have been prescribed as the standard treatment for osteoporosis (Bellido & Plotkin, 2011; Ruan et al., 2012; Briot & Roux, 2015). Bisphosphonates, such as risedronate and alendronate, are a class of drugs that directly limits bone loss by inhibiting osteoclast-mediated bone resorption and by inducing osteoclast apoptosis (Rogers et al., 2011; Russell, 2011). There is evidence that alendronate is effective in stimulating bone mineral density, even when osteoporosis had already progressed to an advanced degree (Rogers et al., 2011; Khosla et al., 2012). Statins, which act via different mechanisms, have recently been proposed to treat osteoporosis and prevent fractures (Dimic et al., 2010; Zhang et al., 2014; Oryan et al., 2015). Simvastatin, a 3-hydroxy-3-methylglutaryl coenzyme A reductase inhibitor, is clinically used to reduce blood cholesterol levels (Ruan et al., 2012; Dai et al., 2016). This drug is known to affect bone metabolism and to suppress osteoclastogenesis by inhibiting the receptor of activator of NF-$\kappa\beta$ ligand (RANKL)-induced NF-κB activation pathway, a pivotal metabolic pathway that is involved in the pathogenesis of bone-loss-related diseases (Nakashima & Haneji, 2013; Zhang et al., 2014; Oryan et al., 2015). Simvastatin appears to increase bone formation by inhibiting matrix metalloproteinase expression and by promoting osteoblast differentiation and bone mineralization (Ruan et al., 2012; Dai et al., 2016).

Considering that drugs used to restrict bone loss or to stimulate bone development are not always successful, there is an urgent need for the development of more effective drugs and for rational therapeutic schemes to be applied in the treatment of metabolically determined bone diseases. Currently, studies comparing the combined effects of bisphosphonates and statins on bone structure and function remain scarce (Tanriverdi et al., 2005; Nagashima et al., 2012). Thus, considering that these drugs can interact in a synergistic way to modulate bone metabolism (Russell, 2011), we used a murine model of dexamethasone-induced osteoporosis to investigate the effects of different therapeutic schemes combining sodium alendronate and simvastatin on bone mineral and protein composition, microstructural remodeling, and mechanical function.

Materials and Methods

Animals and Treatments

In total, 56 Wistar rats obtained from the University Federal de Viçosa (UFV) were randomized into eight groups with seven animals each. G1 (control): non-osteoporotic animals treated with 0.5 mL of 0.9% saline solution; G2 (osteoporosis group): osteoporotic animals treated with 0.5 mL of 0.9% saline solution; G3, G4, and G5: osteoporotic animals treated with 0.2, 0.4, and 0.8 mg/kg sodium alendronate, respectively; G6: osteoporotic animals treated with sodium alendronate (0.2 mg/kg) plus simvastatin (0.4 mg/kg); G7: osteoporotic animals treated with sodium alendronate (0.4 mg/kg) plus simvastatin (0.6 mg/kg); and G8: osteoporotic animals treated with sodium alendronate (0.8 mg/kg) plus simvastatin (1 mg/kg). The dosages of alendronate (Sunyecz, 2008) and simvastatin (Ribeiro et al., 2013) were determined according to the recommendation for humans. Osteoporosis was induced by intramuscular injection of dexamethasone disodium phosphate (7 mg/kg; ACHE, Guarulhos, SP, Brazil) once a week for 5 weeks (Lucinda et al., 2013). After osteoporosis induction, the treatments were diluted in 1 mL of 0.9% saline solution and were administered daily by gavage for 8 weeks. During the experiment, the animals were kept in individual cages at room temperature (23 ± 2°C), relative air humidity of 60–70%, and a 12 h–12 h light–dark cycle, with food and water *ad libitum*. The institutional Ethics Committee approved all experimental procedures (approval protocol no. 014/2008).

Biochemical Analysis of Serum

At 8 weeks of treatment, the animals were euthanized by cardiac puncture after anesthesia (180 mg/kg ketamine and 10 mg/kg xylazine, i.p.). Immediately, 4 mL of blood was collected to determine the following parameters in the serum by using commercial diagnostic kits (Bioclin, Belo Horizonte, MG, Brazil): calcium, phosphorus, glucose, alkaline phosphatase (ALP), urea, total protein, total cholesterol, and triglycerides. The collected blood was also analyzed using an automated hematology analyzer (Human Count, São Paulo, SP, Brazil) (Sequetto et al., 2013).

Bone Biomechanical Assay

The right femurs were removed and submitted to the three-point bending test until complete fracture at a velocity of 3 mm/min (Soares et al., 2015). A universal mechanical testing system (MTS) with a load cell of 10,00 kgf was used (5966 Dual Column Tabletop Model testing system; Instron, Grove City, PA, USA). The radius of the upper point and the radius and distance of the two lower supports was 0.5 mm. Each femur was tested in the anteroposterior plane (concave-up position), with the anterior surface of the bone facing upwards. The load and displacement data were obtained directly from the MTS and recorded with a computer coupled to the testing machine. These data were used for the acquisition and calculation of the maximum load, displacement at maximum load, and extrinsic stiffness. The extrinsic stiffness was calculated as the slope of the linear portion of the elastic region of the load-displacement curve (Soares et al., 2015).

Energy-Dispersive X-ray Spectroscopy

The tissue content and distribution of minerals in the compact bone (diaphysis) and cancellous bone (distal epiphyses) of the femur was investigated by energy-dispersive X-ray spectroscopy (EDS) using a scanning electron microscope

(LEO 1430VP; Carl Zeiss, Oberkochen, Germany) with an attached X-ray detection system (Tracor TN5502, Tracor Northern Inc., Middleton, WI, USA) according to Novaes et al. (2013) and Cupertino et al. (2017). In brief, bone fragments were fixed (2.5% glutaraldehyde, 0.2% picric acid, 3% sucrose, and 5 mM $CaCl_2$ in 0.1 M sodium cacodylate buffer, pH 7.2), dehydrated in ethanol, submitted to critical point drying (CPD030; Bal-tec, Witten, North Rhine-Westphalia, Germany), and covered with carbon. The EDS microanalysis was examined from one central and five peripheral areas for both fragments of the diaphysis and epiphyses. This analysis was performed at ×600 on-screen magnification, an accelerating voltage of 20 kV, and a working distance of 19 mm. Thus, for each group the total area of the diaphysis and epiphyses investigated was 37.12×10^4 and $12.37 \times 10^4\ \mu m^2$, respectively. The proportion of the elements carbon (C), nitrogen (N), oxygen (O), potassium (K), phosphorus (P), sodium (Na), calcium (Ca), and magnesium (Mg) were measured by EDS, and are expressed as a mean value for all diaphysis and epiphyses areas analyzed.

Atomic Absorption Spectrometry

Fragments of the diaphysis that were not used in the microscopic analysis were weighed on an analytical balance and incubated at 70°C until they reached dry constant weight. The pre-dried samples were digested in an Erlenmeyer flask using 1.5 mL of concentrated HNO_3 and 0.5 mL of 70% $HClO_4$. The temperature of the digestion solution was gradually increased on a heating plate from 70 to 90°C over 30 min. After the dilution of the digested material, the concentrations of calcium and phosphorus were determined by atomic absorption spectrometry (Cupertino et al., 2013).

Biochemical Analysis of Collagenous and non-Collagenous Proteins in Bone Tissue

Samples of bone diaphysis were defatted with petroleum ether for 10 h, dried, weighed, and demineralized using ethylenediaminetetraacetic acid (EDTA) disodium salt solution (0.5 M, pH 8.2). The content of soluble non-collagenous proteins in EDTA extract was determined by the Bradford method using bovine albumin as the reference (Bradford, 1976). To determine tissue levels of collagenous proteins, demineralized bone samples were washed with deionized water to remove EDTA and dried at 80°C for 16 h. The samples were immersed in a digestion solution (0.5 mL H_2SO_4, 5 g copper sulfate, 0.5 g selenium, 50 g potassium sulfate) at 380°C for 3 h. Next, 50 μL of this solution was diluted in 50 μL of acid water (2 mL H_2SO_4 in 75 mL deionized water) and incubated with 1 mL of a developer solution (0.5 g EDTA, 0.5 g phenol crystal, and 2.5 mg sodium nitroprusside in 50 mL of distilled and deionized water, 0.25 g NaOH, 0.19 g Na_2HPO_4, 1.59 g $Na_3PO_4.12H_2O$, and 2 mL of sodium hypochlorite in deionized water). Samples (50 μL) were analyzed in a spectrophotometer at 630 nm and compared with a blank solution (2 mL H_2SO_4, 50 mg $(NH_4)_2SO_4$ in 75 mL deionized water). The content of collagenous proteins was obtained by multiplying the nitrogen level by the correction factor 6.25 (Moraes et al., 2010).

Scanning Electron Microscopy and Compact Bone Morphology

After the bone biomechanical test, fragments of femur diaphysis and distal epiphyses were fixed in histological fixative (2.5% glutaraldehyde, 0.2% picric acid, 3% sucrose, and 5 mM $CaCl_2$ in 0.1 M sodium cacodylate buffer, pH 7.2) for 48 h at 4°C. Then, the fixed samples were dehydrated in ethanol, and submitted to critical point drying (Novaes et al., 2013). The diaphysis and epiphyses were longitudinally fractured, covered with carbon and observed in a scanning electron microscope (LEO 1430VP, Carl Zeiss, Oberkochen, Germany). The porosity of the diaphysis cortical bone was evaluated by determining the number of pores per histological area (N[*pores*], N/mm^2) and the proportion of the tissue occupied by pores (Vv[pores], %) from the internal shaft surface. The number of pores was determined according to the formula:

$$N[pores] = Q^{-}[pores] / A_T, \quad (1)$$

where Q^{-}[pores] is the number of pores inside an unbiased two-dimensional test area (A_T) of $4.12 \times 10^4\ \mu m^2$ at tissue level. The proportion of pores was determined according to the formula:

$$Vv[pores] = \Sigma P_P[pores] / \Sigma P_T, \quad (2)$$

where ΣP_P[pores] is the number of points that hit the pores and ΣP_T the total number of test points, here 77 (Mandarim-de-Lacerda, 2003). Bone fragments obtained from the proximal, mean, and distal femur diaphysis were analyzed. For each animal and diaphysis segment, five randomly sampled fields (magnification 250×) and a total bone area of $46.4 \times 10^5\ \mu m^2$ were analyzed for each group.

Histopathological Processing and Cancellous Bone Morphology

The distal epiphyses used for mineral microanalysis were decalcified by immersion in a neutral decalcification solution (14% EDTA, pH 7.0) for 30 days. Then, the epiphyses were rinsed in distilled water, dehydrated in ethanol, cleared in xylol, and embedded in paraffin in a vertical orientation relative to the longitudinal femur axis. Blocks were cut into 4-μm-thick histological sections, stained with hematoxylin–eosin, and mounted on histology slides. To avoid repeated analysis of the same histological area, sections were evaluated in semi-series, using one in every 20 sections. The slides were visualized using a 40× objective lens and histological images were captured using a light microscope (Olympus BX-60®, Tóquio, Japan) connected to a digital camera (Olympus QColor-3®) (Sequetto et al., 2014).

The volume density occupied by trabecular bone (Vv[*bone*], %) was estimated by point counting according to equation (2) (Mandarim-de-Lacerda, 2003). A test system of 42 points was used in a test area (A_T) of $1.38 \times 10^4\ \mu m^2$ at

tissue level. In total, 70 randomly sampled microscopic fields (magnification 400×) and a total bone area of $96.6 \times 10^4\,\mu m^2$ were analyzed for each group. Trabecular connectivity was estimated using the principle of marrow star volume (V*marrow), which is defined as the mean volume of all the parts of an object when seen unobscured along uninterrupted straight lines in all directions from random points inside the object. In cancellous bone, V*marrow provides an estimate of the mean size of the marrow space in three-dimensions and reflects connectivity. V*marrow was calculated as follows:

$$V^*marrow = (\pi / 3) \times \ell^3, \quad (3)$$

where ℓ is the average length of an intercept with random orientation through a random point (Cruz-Orive et al., 1992). Vv and V*marrow were estimated from the same microscopic image. Trabecular thickness was estimated using a variant of the sphere-fitting method based on 3D calculations. The basic approach is to determine the diameter of the largest possible circle that can be fitted while completely contained within the bone trabecula and then to average these diameters (Bouxsein et al., 2010). The surface density of bone trabeculae was estimated according to the following formula:

$$Sv[bt] = (2 \times \Sigma I[bt]) / L_T, \quad (4)$$

where $\Sigma I[bt]$ represents the total number of intersections between the cycloid arcs (i.e., 12) and the surface of bone trabeculae, and L_T is the total length of the cycloid arcs system (i.e., 1220 μm) (Mandarim-de-Lacerda, 2003).

Statistical Analysis

The normality of the data distribution was verified by the D'agostino–Pearson test. Data with parametric distribution were expressed as mean and standard deviation (mean ± SD) and nonparametric data were represented as mean and interquartile range. The biochemical and mineral data were analyzed using one-way analysis of variance, followed by the Tukey's *post hoc* test. The histomorphometric data were compared using the Kruskal–Wallis test. $p < 0.05$ was regarded as significant.

Results

Biochemical Analysis of Serum

Levels of ALP in serum were lower in the groups that received the two highest doses of alendronate (G4 and G5), and also in groups that received the combined treatment with alendronate and simvastatin (G6, G7, and G8) compared with the non-osteoporotic control animals (G1). The amount of phosphorus in serum was lower in the groups treated with higher doses of alendronate and simvastatin (G8) when compared with the osteoporotic control group (G2). The content of calcium was higher in G2, G3, and G4 compared with the G1 (control) (Table 1).

Bone Biomechanical Assay

Compared to non-osteoporotic control animals (G1), the ability to withstand maximum load was lower in the osteoporotic groups (G2, G3, and G4), and was increased in the groups receiving sodium alendronate and simvastatin in increasing doses (G6, G7, and G8, respectively). G5 also showed a higher load-bearing capacity when compared with G2, G3, and G4. Groups treated with higher doses of alendronate (G5), and groups that received higher doses of alendronate associated with simvastatin (G7 and G8), showed increased bone stiffness compared with the groups G3, G4, and G6 (Table 2).

Distribution of Chemical Elements in Compact and Cancellous Bone

In the same group, the distribution of chemical elements was similar when comparing compact and cancellous bone (data not shown). The group that received alendronate and simvastatin in higher doses (G8) showed similar values of C and O to those found in G1. The amount of calcium and

Table 1. Serum Biochemical Parameters in Osteoporotic Rats Treated with Sodium Alendronate and Simvastatin.

Parameters (mg/dL)	G1	G2	G3	G4	G5	G6	G7	G8
ALP	57.0 ± 6.0^a	77.7 ± 6.3^b	70.6 ± 5.1^b	56.2 ± 5.5^a	57.5 ± 4.9^a	54.6 ± 5.8^a	55.9 ± 5.2^a	59.7 ± 5.0^a
Calcium	8.6 ± 1.0^a	10.7 ± 0.8^b	10.9 ± 0.6^b	10.6 ± 0.5^b	9.3 ± 0.7^{ab}	9.6 ± 0.5^{ab}	9.5 ± 0.7^{ab}	9.6 ± 0.6^{ab}
Phosphorus	6.2 ± 0.4^a	8.9 ± 0.8^b	8.7 ± 0.9^b	8.4 ± 0.5^b	7.5 ± 0.7^{bc}	7.7 ± 0.6^{bc}	7.8 ± 0.6^{bc}	6.9 ± 0.7^{ac}
Glucose	135.1 ± 11.6^a	146.8 ± 17.9^a	132.0 ± 15.1^a	136.8 ± 14.6^a	154.6 ± 15.2^a	147.2 ± 16.0^a	162.5 ± 11.9^a	160.9 ± 17.1^a
T. protein	71.5 ± 3.1^a	71.8 ± 6.5^a	78.4 ± 4.2^a	72.6 ± 4.9^a	72.4 ± 3.8^a	78.8 ± 4.0^a	76.6 ± 4.3^a	77.5 ± 4.5^a
T. cholesterol	125.4 ± 9.2^a	101.2 ± 11.8^a	106.3 ± 10.4^a	103.0 ± 12.5^a	108.1 ± 10.7^a	117.3 ± 11.3^a	112.4 ± 14.8^a	115.2 ± 13.5^a
Triglycerides	56.4 ± 5.9^a	54.5 ± 7.2^a	56.6 ± 6.1^a	58.1 ± 7.7^a	60.7 ± 6.9^a	59.5 ± 8.0^a	54.1 ± 6.5^a	59.6 ± 6.0^a
Urea	24.4 ± 3.2^a	35.7 ± 5.6^b	35.9 ± 4.8^b	34.7 ± 4.0^b	35.2 ± 3.3^b	35.2 ± 4.6^b	25.7 ± 3.0^a	26.1 ± 3.8^a

The data are expressed as mean ± SD.

G1, non-osteoporotic; G2, osteoporotic; G3, G4, and G5, osteoporotic treated with sodium alendronate (0.2, 0.4, and 0.8 mg/kg, respectively); G6, G7, and G8, osteoporotic treated with sodium alendronate (0.2, 0.4, and 0.8 mg/kg, respectively) combined with simvastatin (0.4, 0.6, and 1 mg/kg, respectively); ALP, alkaline phosphatase; T. protein, total protein; T. cholesterol, total cholesterol.

[a,b,c]Different superscript letters in the rows indicates statistical difference between groups ($p < 0.05$).

Table 2. Biomechanical Properties of Bone Tissue from Osteoporotic Rats Treated with Sodium Alendronate and Simvastatin.

Groups	Maximum load (N)	Displacement (mm)	Stiffness (N/mm)
G1	26.13 ± 1.28^{a}	0.24 ± 0.03^{a}	297.30 ± 36.21^{a}
G2	16.02 ± 2.46^{b}	0.32 ± 0.10^{a}	104.45 ± 40.28^{b}
G3	16.59 ± 2.09^{b}	0.30 ± 0.08^{a}	125.33 ± 36.19^{b}
G4	17.45 ± 2.11^{b}	0.29 ± 0.08^{a}	132.92 ± 34.85^{b}
G5	21.83 ± 1.75^{c}	0.27 ± 0.09^{a}	211.37 ± 30.09^{c}
G6	19.33 ± 2.00^{bc}	0.30 ± 1.0^{a}	153.61 ± 25.11^{b}
G7	24.15 ± 1.61^{ac}	0.27 ± 0.07^{a}	223.18 ± 29.40^{c}
G8	24.97 ± 1.74^{ac}	0.28 ± 0.05^{a}	250.72 ± 30.83^{ac}

Data are expressed as mean and standard deviation (mean ± SD).
G1, non-osteoporotic; G2, osteoporotic; G3, G4, and G5, osteoporotic treated with sodium alendronate (0.2, 0.4, and 0.8 mg/kg, respectively); G6, G7, and G8, osteoporotic treated with sodium alendronate (0.2, 0.4, and 0.8 mg/kg, respectively) combined with simvastatin (0.4, 0.6, and 1 mg/kg, respectively).
[a,b,c]Different superscript letters in the columns indicates statistical difference between groups ($p < 0.05$) for each chemical element.

phosphorus was lower in osteoporotic groups (G2, G3, and G4) compared with G1, which presented similar values compared with those groups that received sodium alendronate and simvastatin in increasing doses (G6, G7, and G8). The G5 group also showed similar calcium and phosphorus levels compared with G1 animals (Fig. 1).

Calcium, Phosphorus, and Protein Levels in Compact Bone

Bone content of calcium, phosphorus, and non-collagenous and collagenous proteins was drastically reduced in osteoporotic groups (G2, G3, and G4) compared with the non-osteoporotic control group (G1). These parameters were significantly increased in the groups treated with the higher doses of alendronate and simvastatin (G7 and G8) compared with other osteoporotic groups (Table 3). In G8, all parameters were similar to G1 animals.

Bone Porosity, Trabecular Thickness, and Surface Area

Figure 2 shows photomicrographs of the femoral diaphysis, where Figures 2a and 2b show the pores distribution in osteoporoic bone, and Figures 2c and 2d show the pores distribution in a non-osteoporotic bone. The number of pores per histological area (Fig. 2e) and the proportion of the bone tissue occupied by pores (Fig. 2f) in the osteoporotic groups (G2, G3, G4, and G6) was higher when compared with the osteoporotic groups (G5, G7, and G8). The group

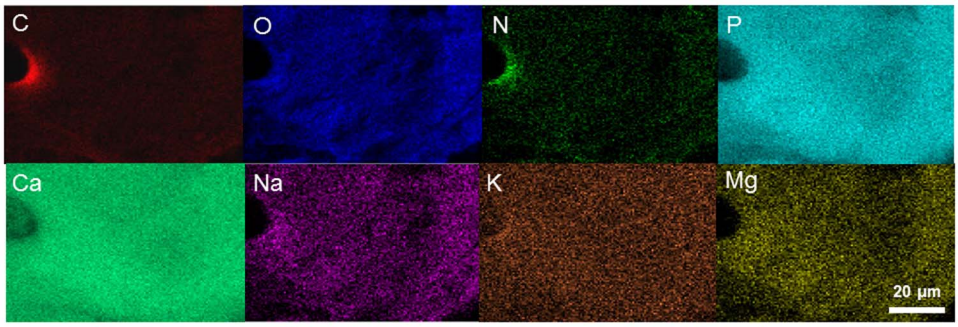

Element	G1	G2	G3	G4	G5	G6	G7	G8
C	18.82 ± 3.27^{a}	28.75 ± 4.15^{b}	28.53 ± 4.08^{b}	27.81 ± 4.33^{b}	$22.64 \pm 4.37^{a,b}$	$22.24 \pm 4.11^{a,b}$	$21.11 \pm 4.08^{a,b}$	20.10 ± 3.17^{a}
O	17.13 ± 3.38^{a}	26.81 ± 4.73^{b}	24.48 ± 4.01^{b}	23.86 ± 3.60^{b}	$20.51 \pm 4.12^{a,b}$	$20.02 \pm 4.20^{a,b}$	$19.04 \pm 4.16^{a,b}$	18.44 ± 3.09^{a}
N	5.61 ± 1.03	6.70 ± 1.55	6.85 ± 1.38	6.93 ± 1.29	6.27 ± 1.35	6.18 ± 1.16	6.69 ± 1.07	5.97 ± 1.14
P	21.75 ± 2.11^{a}	12.69 ± 2.40^{b}	13.87 ± 2.09^{b}	14.50 ± 2.01^{b}	18.93 ± 2.19^{a}	19.36 ± 2.21^{a}	19.82 ± 1.75^{a}	20.91 ± 2.00^{a}
Ca	35.92 ± 2.75^{a}	24.12 ± 2.25^{b}	25.39 ± 1.99^{b}	26.01 ± 2.13^{b}	30.77 ± 2.31^{a}	31.29 ± 2.24^{a}	32.49 ± 2.58^{a}	33.73 ± 2.19^{a}
Na	0.20 ± 0.09	0.28 ± 0.09	0.31 ± 0.11	0.25 ± 0.10	0.29 ± 0.10	0.28 ± 0.09	0.26 ± 0.08	0.23 ± 0.08
K	0.04 ± 0.01	0.05 ± 0.01	0.07 ± 0.02	0.06 ± 0.01	0.04 ± 0.01	0.06 ± 0.01	0.05 ± 0.01	0.05 ± 0.01
Mg	0.53 ± 0.10	0.60 ± 0.11	0.50 ± 0.10	0.58 ± 0.10	0.55 ± 0.10	0.57 ± 0.10	0.54 ± 0.09	0.57 ± 0.10

Figure 1. Mineral content in bone tissue from osteoporotic rats treated with sodium alendronate and simvastatin analyzed by energy-dispersive X-ray spectroscopy. The image represents the distribution of carbon (C), nitrogen (N), oxygen (O), potassium (K), phosphorus (P), sodium (Na), calcium (Ca), and magnesium (Mg) in the compact bone of an animal in the Group 1. The table shows the percentage (%) of chemical elements in both compact and trabecular bone for each group (mean ± SD). [a,b]Different superscript letters in the lines indicates statistical difference between groups ($p < 0.05$) for each chemical element. G1, non-osteoporotic; G2, osteoporotic; G3, G4, and G5, osteoporotic treated with sodium alendronate (0.2, 0.4, and 0.8 mg/kg, respectively); G6, G7, and G8, osteoporotic treated with sodium alendronate (0.2, 0.4, and 0.8 mg/kg) combined with simvastatin (0.4, 0.6, and 1 mg/kg, respectively).

Table 3. Calcium, Phosphorus and Protein Content in Bone Tissue from Osteoporotic Rats Treated with Sodium Alendronate and Simvastatin Analyzed by Atomic Absorption Spectrometry.

Groups	Ca (mg/g)	P (mg/g)	Ca/P ratio	NCP (mg/g)	CP
G1	214.39 ± 9.11^{a}	100.07 ± 5.58^{a}	2.21 ± 0.23	7.32 ± 0.48^{a}	32.52 ± 3.17^{a}
G2	150.26 ± 10.55^{b}	70.15 ± 6.29^{b}	2.14 ± 0.47	4.19 ± 0.55^{b}	18.46 ± 3.25^{b}
G3	156.07 ± 9.14^{b}	71.66 ± 4.47^{b}	2.18 ± 0.36	4.31 ± 0.60^{b}	19.50 ± 3.33^{b}
G4	161.60 ± 9.25^{b}	76.39 ± 4.03^{b}	2.12 ± 0.31	4.61 ± 0.39^{b}	19.08 ± 3.11^{b}
G5	185.32 ± 8.11^{c}	87.43 ± 4.11^{c}	2.12 ± 0.28	5.95 ± 0.41^{c}	22.16 ± 3.70^{bc}
G6	189.47 ± 10.28^{c}	87.19 ± 5.00^{c}	2.17 ± 0.40	6.11 ± 0.50^{c}	26.15 ± 3.09^{cd}
G7	197.51 ± 8.90^{ac}	90.27 ± 5.12^{ac}	2.19 ± 0.34	6.57 ± 0.59^{cd}	29.53 ± 3.19^{cd}
G8	210.64 ± 9.73^{ac}	94.52 ± 4.61^{ac}	2.23 ± 0.28	7.19 ± 0.43^{ad}	31.77 ± 3.05^{ad}

Data are expressed as mean and standard deviation (mean ± SD).
Ca, calcium; P, phosphorus; NCP, non-collagenous proteins; CP, collagenous proteins; G1, non-osteoporotic; G2, osteoporotic; G3, G4 and G5, osteoporotic treated with sodium alendronate (0.2, 0.4, and 0.8 mg/kg, respectively); G6, G7, and G8, osteoporotic treated with sodium alendronate (0.2, 0.4, and 0.8 mg/kg, respectively) combined with simvastatin (0.4, 0.6, and 1 mg/kg, respectively).
^{a,b,c,d}Different superscript letters in the columns indicates statistical difference between groups ($p < 0.05$) for each chemical element.

receiving the higher doses of alendronate and simvastatin together (G8) presented similar pores distribution compared with G1 animals.

Figure 3 shows photomicrographs of the femoral epiphysis. From a qualitative analysis, groups G2, G3, and G4 had evident trabecular narrowing and reciprocal marrow space expansion compared with the other groups. In the groups that were treated with increasing doses of alendronate and simvastatin (G6, G7, and G8, respectively), marrow space and trabecular structures presented marked

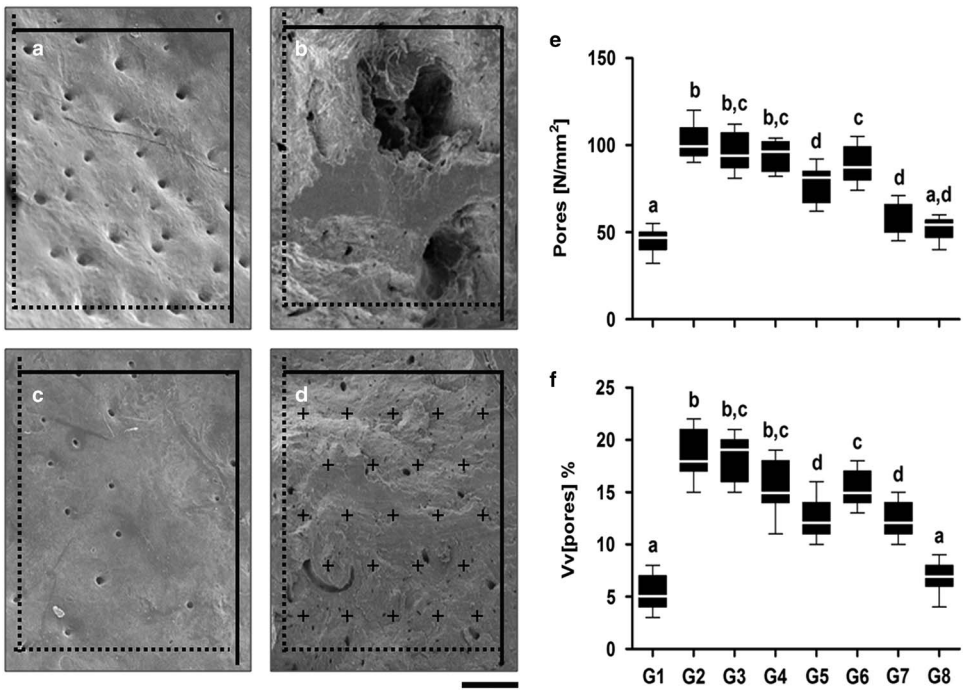

Figure 2. Morphological parameters of the femoral diaphysis in osteoporotic rats treated with sodium alendronate (SA) and simvastatin (SI). **a–d:** Representation of the method applied to determine de number and proportion of pores in the bone diaphysis using scanning electron micrographs (bar = 100 μm). **d:** Represented the test system used in the counts, which was composed by an unbiased bi-dimension test frame of known area associated with test points. Note the difference in the number and size of pores between the osteoporotic (**a** and **b**) and control animals (**c** and **d**). The number (**e**) and volume density—Vv (**f**) of pores per histological area are represented in the graphics. In **e** and **f**, the box represents the interquartile interval with the median indicated (horizontal line), and whiskers represent the superior and inferior quartiles. ^{a,b,c,d}Different letters in the columns denotes statistical difference between groups ($p < 0.05$). G1, control: 0.9% saline; G2, control dexamethasone-induced osteoporosis: 0.5 mL of 0.9% saline; G3, G4, and G5, osteoporotic animals treated with SA (0.2, 0.4, and 0.8 mg/kg, respectively); G6, G7, and G8, osteoporotic treated with SA (0.2, 0.4, and 0.8 mg/kg) combined with simvastatin (0.4, 0.6, and 1 mg/kg, respectively).

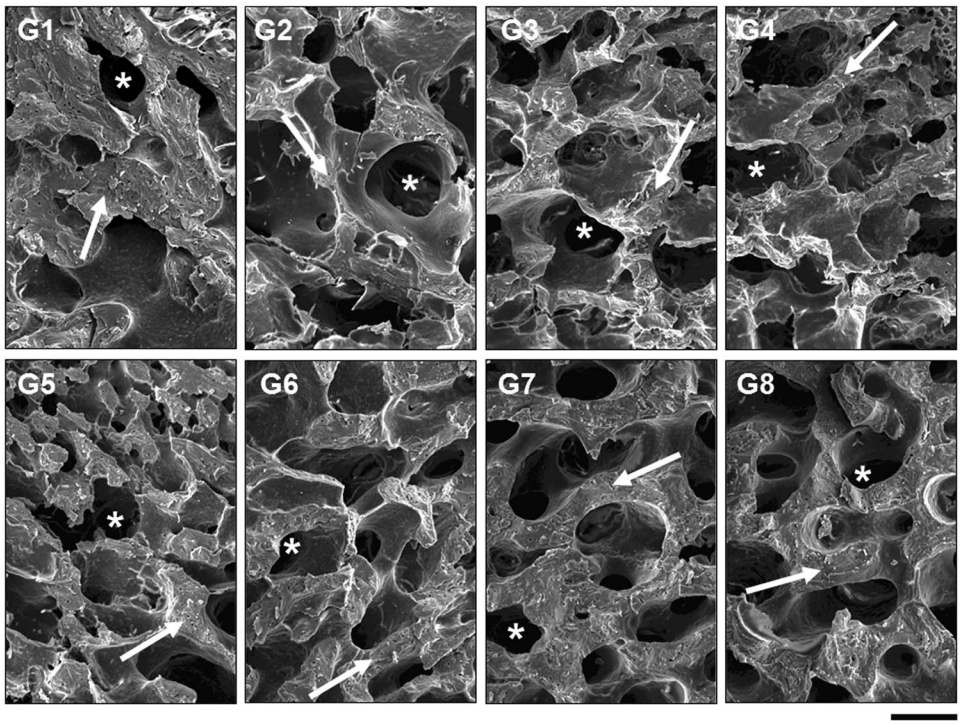

Figure 3. Representative scanning electron micrographs of the femoral epiphysis from osteoporotic rats treated with sodium alendronate and simvastatin. Arrow: bone trabecula; asterisk: marrow space; G1, non-osteoporotic; G2, osteoporotic; G3, G4, and G5, osteoporotic treated with sodium alendronate (0.2, 0.4, and 0.8 mg/kg, respectively); G6, G7, and G8, osteoporotic treated with sodium alendronate (0.2, 0.4, and 0.8 mg/kg) combined with simvastatin (0.4, 0.6, and 1 mg/kg, respectively).

attenuation of the morphological alterations compared with the groups G2, G3, and G4.

Figures 4 to 6 shows fragments of the distal epiphysis of decalcified bones. The G1 group had thick trabecular bone (i.e., Vv, Sv, and trabecular thickness) with a small medullary space (V*marrow) compared with the groups G2–G7. The group G2 showed the most reduced area of trabecular bone and an increased medullar region compared with the other groups, except G3. The best results were observed in the group receiving the higher doses of alendronate and simvastatin together (G8), which presented similar bone marrow volume, trabecular distribution, thickness, and surface area compared with G1 animals.

Discussion

In the experimental model investigated, animals treated with dexamethasone presented increased serum levels of ALP, calcium, phosphorus, and urea. All these parameters were attenuated in the groups receiving the combined treatment with alendronate and simvastatin, especially in the highest doses tested. Here, ALP levels were useful indicators of severe osteoporosis, but were not applicable in the groups with moderate or low bone loss. Thus, it is possible that due to the non-specificity of ALP, changes in circulating levels of this enzyme determined by disturbances in bone metabolism are detectable only in extreme conditions of bone injury. As ALP is synthesized in several organs, serum levels of this enzyme represent a non-specific marker of bone metabolism, and are therefore, a controversial indicator of therapeutic efficacy in bone diseases (Wheater et al., 2013; Hlaing & Compston, 2014). However, changes in circulating levels of ALP have been observed in humans and animals with bone disorders, including osteoporosis (Garnero, 2008; Vasikaran et al., 2011). As ALP is an enzyme that is present in osteoblast membranes, increased circulating levels of ALP may indicate membrane disruption and osteoblast death (Vasikaran et al., 2011; Wheater et al., 2013), which are typically observed in glucocorticoid-induced osteoporosis (Weinstein, 2012; Whittier & Saag, 2016).

Since bone tissue is the main calcium and phosphorus reservoir (i.e., hydroxyapatite crystals), circulating levels of these minerals have been consistently used to investigate the balance between osteogenesis and osteolysis (Rosenson et al., 2005; Kourkoumelis et al., 2012; Hlaing & Compston, 2014). Here, calcium and phosphorus serum levels were high in non-treated animals exposed to dexamethasone, whereas those treated with the highest doses of alendronate and simvastatin presented similar levels compared with control animals. This finding indicates that the mineral dynamics was impaired by dexamethasone, but this effect was antagonized especially when alendronate and simvastatin were combined, thus changing mineral metabolism in favor of osteogenesis. Reduced bone mineral mass has been

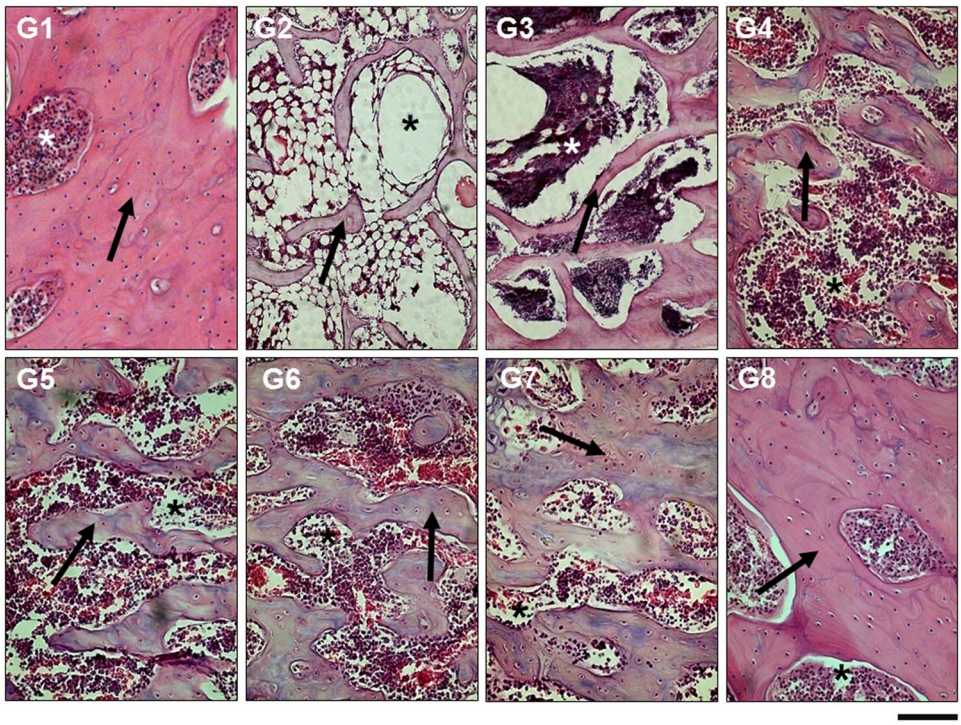

Figure 4. Representative photomicrography of the epiphysis from osteoporotic rats treated with sodium alendronate and simvastatin. Arrow: bone trabecula; asterisk: marrow space; G1, non-osteoporotic; G2, osteoporotic; G3, G4, and G5, osteoporotic treated with sodium alendronate (0.2, 0.4, and 0.8 mg/kg, respectively); G6, G7, and G8, osteoporotic treated with sodium alendronate (0.2, 0.4, and 0.8 mg/kg, respectively) combined with simvastatin (0.4, 0.6, and 1 mg/kg, respectively).

associated with increased calcium and phosphorus serum levels during prolonged glucocorticoid treatment. This effect cannot be associated with increased intestinal mineral absorption or depressed renal clearance, as they are, respectively, reduced and enhanced by glucocorticoids in both humans and animals (Manelli & Giustina, 2000; Sasaki et al., 2001). Thus, increased mineral serum levels seem to be a direct result of an osteolytic bone response rather than a disturbance in secondary organs involved in systemic mineral balance. In glucocorticoid-induced osteoporosis, mineral disturbances are mainly the result of reduced osteoblast activity and upregulation of osteoclastogenesis and osteolysis, which stimulates bone matrix resorption and mineral release in blood (Briot & Roux, 2015; Whittier & Saag, 2016).

Several physiopathological studies explain the rational basis by with glucocorticoids induce osteolysis and bone fragility (Manelli & Giustina, 2000; Miller et al., 2000; Weinstein, 2012; Briot & Roux, 2015). There is consistent evidence that glucocorticoids, including dexamethasone, decrease osteoblast differentiation, maturation, and function, and induce cell apoptosis (Hurson et al., 2007; Ruan et al., 2012; Briot & Roux, 2015). These steroidal drugs also increase the expression of growth factors, such as granulocyte-macrophage colony-stimulating factor and RANKL, which are both involved in osteoclast differentiation and increased cell survival, while at the same time reducing osteoblastic expression of osteoprotegerin (Briot & Roux, 2015; Whittier & Saag, 2016). Bone metabolism is even more impaired due to a reduction in bone neoangiogenesis, as glucocorticoids inhibit vascular endothelial growth factor (VEGF) expression, tissue hydration, nutrition, and growth (Weinstein, 2012; Briot & Roux, 2015).

Considering the pathogenesis of dexamethasone-induced osteoporosis, it is clear that all molecular events triggered by glucocorticoids overcome the protective osteogenic mechanisms in favor of osteolysis, with a negative impact on tissue mechanics and resistance to fracture (Weinstein, 2001; Mclaughlin et al., 2002; Whittier & Saag, 2016). We observed that in non-treated animals receiving dexamethasone, there was marked mechanical fragility in compact and cancellous bone, which was accompanied by extensive bone structural remodeling, as well as reduced protein and mineral tissue levels. However, alendronate and simvastatin, especially when combined, improved bone mechanical function, such as the maximum load and stiffness, at the same time that they improved inorganic and organic bone mass in a dose-dependent fashion. Mineral homeostasis is critical to bone structure and mechanical behavior (Weiner & Wagner, 1998; Soares et al., 2015, Zimmermann et al., 2015). Due to the co-dependent relationship between calcium and phosphorus in constructing the fundamental crystalline structure of the mineral bone matrix (i.e., hydroxyapatite crystals), the relative and

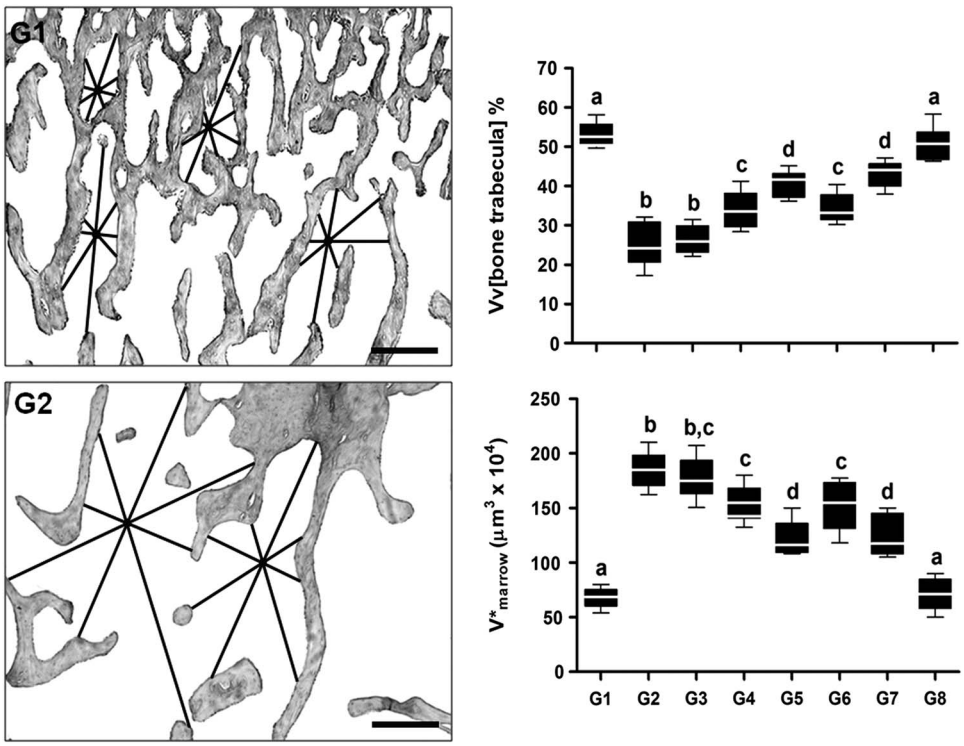

Figure 5. Volume density of trabecular bone and bone marrow star volume (V*marrow) in osteoporotic rats treated with sodium alendronate and simvastatin. The photomicrography's (G1 and G2) are representative of V*marrow concept (hematoxylin–eosin staining, bar = 40 μm). In the graphics, the box represents the interquartile interval with the median indicated (horizontal line), and whiskers represent the superior and inferior quartiles. [a,b,c,d]Different letters in the columns denotes statistical difference between groups ($p < 0.05$). Vv, volume density; G1, non-osteoporotic; G2, osteoporotic; G3, G4, and G5, osteoporotic treated with sodium alendronate (0.2, 0.4, and 0.8 mg/kg, respectively); G6, G7, and G8, osteoporotic treated with sodium alendronate (0.2, 0.4, and 0.8 mg/kg) combined with simvastatin (0.4, 0.6, and 1 mg/kg, respectively).

absolute contents of both minerals are essential biomarkers to evaluate bone health and therapeutic efficacy (Weiner & Wagner, 1998; Kourkoumelis et al., 2012). However, although bone proteins are frequently neglected in several studies, these molecules form the morphofunctional basis that modulates bone growth and mineralization (Grynpas et al., 1994; Garnero, 2008). Here, the highest doses of alendronate and simvastatin were effective in restoring bone levels of non-collagenous and collagenous proteins, indicating a positive osteogenic effect, in which the structuration of the organic extracellular matrix (i.e., osteoid) is an invariable requirement to the increase in bone mineralization and mechanical resistance (Grynpas et al., 1994; Garnero, 2008). Serum biochemistry reinforced these findings, since animals receiving the highest doses of alendronate and simvastatin presented reduced urea serum levels, a systemic indicator of protein catabolism. In glucocorticoid-induced osteoporosis, the progressive depletion of the organic and inorganic bone matrix is a pivotal determinant of mechanical insufficiency, thus increasing the risk of fractures in humans and animals (Mclaughlin et al., 2002; Kourkoumelis et al., 2012; Weinstein, 2012).

In our study, the volume density and number of pores in compact bone was especially reduced in osteoporotic animals treated with alendronate and simvastatin, indicating that the combined treatment accelerates the microstructural and mechanical bone restoration. This beneficial effect was mainly observed in cancellous bone, in which the marrow space drastically expanded by dexamethasone (i.e., star volume and volume density of the bone trabeculae) was consistently reduced by combined therapy, a finding potentially mediated by osteogenesis and consequent increasing in bone trabeculae thickness. Furthermore, the decreased bone volume observed in glucocorticoid-induced osteoporosis was accompanied by expansion of the marrow adipose tissue. These findings are in accordance with evidence that osteogenic and adipogenic cells arise from a common multipotent precursor (bone marrow stromal cells), which are antagonistically activated in pathways that regulate adipogenesis and osteogenesis (Gimble & Nuttall, 2012; Tsubaki et al., 2012). Therefore, by inhibiting osteogenesis, glucocorticoids modulate several metabolic pathways in favor of adipogenesis. Conversely, by acting as an anabolic bone therapy, alendronate and simvastatin inhibit bone marrow adipogenesis and upregulate osteoblastogenesis (Russell, 2011; Gimble & Nuttall, 2012). Currently, this mechanism has provided an important rational basis that supports the applicability of bisphosphonates and statins in

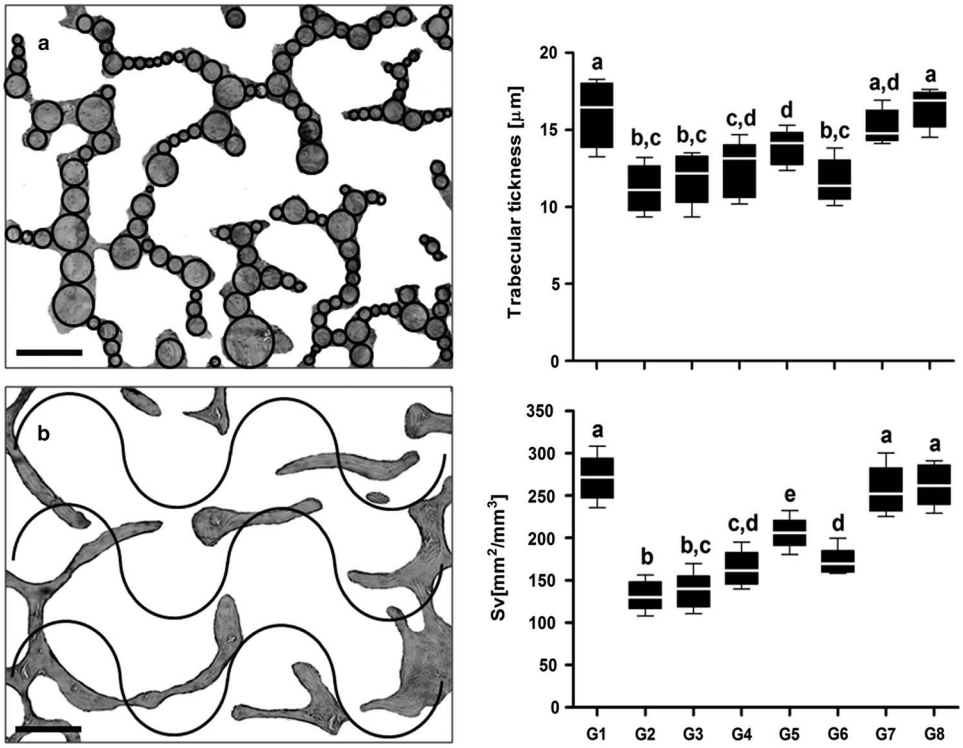

Figure 6. Thickness and surface density (Sv) of trabecular bone in osteoporotic rats treated with sodium alendronate and simvastatin. The photomicrography's represent the methods used to estimate trabecular thickness (**a**) and Sv (**b**) (hematoxylin–eosin staining, bar = 40 μm). In the graphics, the box represents the interquartile interval with the median indicated (horizontal line), and whiskers represent the superior and inferior quartiles. [a,b,c,d,e]Different letters in the columns denotes statistical difference between groups ($p < 0.05$). G1, non-osteoporotic; G2, osteoporotic; G3, G4, and G5, osteoporotic treated with sodium alendronate (0.2, 0.4, and 0.8 mg/kg, respectively); G6, G7, and G8, osteoporotic treated with sodium alendronate (0.2, 0.4, and 0.8 mg/kg) combined with simvastatin (0.4, 0.6, and 1 mg/kg, respectively).

the therapeutic management of osteoporosis (Russell, 2011; Gimble & Nuttall, 2012).

The mechanisms by which bisphosphonates and statins attenuate osteolysis and promote osteogenesis are not completely understood. However, our results are consistent with previous observations that both groups of drugs enhance osteogenesis, thus modulating bone turnover (Rosenson et al., 2005; Xu et al., 2014, Dai et al., 2016). Recent studies indicate that bisphosphonate- and statin-induced bone anabolism may be summarized into three major mechanisms: promotion of osteogenesis, suppression of osteoblast apoptosis, and inhibition of osteoclastogenesis. Apparently, bisphosphonates and statins acts by an additive effect and share an inhibitory modulation on the mevalonate pathway, which has been directly associated with protective bone effects (Bellido & Plotkin, 2011; Rogers et al., 2011; Russell, 2011). In both cases, the synthesis of farnesyl pyrophosphate (FPP) and geranylgeranyl pyrophosphate (GGPP) are dramatically downregulated, favoring the osteogenic pathway (Zhang et al., 2014; Oryan et al., 2015). While FPP and GGPP depletion is mediated by competitive inhibition of the enzyme 3-hydroxy-3-methylglutaryl-coenzyme A reductase by statins, this effect results from the block of FPP synthase activity by bisphosphonates (Ruan et al., 2012; Oryan et al., 2015). Acting as inhibitory molecules, high levels of FPP and GGGP increase the activation of Rho kinase and impair bone formation, as these molecules downregulate the expression of bone morphogenetic protein 2, VEGF, and osteocalcin, and block osteoblastogenesis at the same time as stimulating osteoclast differentiation and osteolysis (Zhang et al., 2014; Oryan et al., 2015).

Specific bone effects are also ascribed to bisphosphonates and statins. Bisphosphonates, such as alendronate, inhibit osteoclast differentiation and function, as well as stimulating cell apoptosis (Bellido & Plotkin, 2011; Nagashima et al., 2012). These effects seem to be prominent in mature osteoclasts, which actively capture large amounts of bisphosphonates, which disrupt the cytoskeleton and mitochondrial membrane integrity, inducing cellular uncoupling from the bone resorption surface and apoptosis by caspase activation (Rogers et al., 2011; Russell, 2011). *In vitro* and *in vivo* studies also indicated that bisphosphonates are able to prevent osteoblast and osteocyte apoptosis induced by glucocorticoids, an effect mediated by the activation of extracellular signal-regulated kinases (ERKs), followed by phosphorylation of the ERK cytoplasmic target, p90RSK kinase, and its substrate C/EBPβ, resulting in increased cell survival (Rogers et al., 2011; Tsubaki et al., 2012).

In addition, the specific anti-osteoclastogenic effect of statins seems to be mediated by induction of increased osteoprotegerin and decreased RANKL mRNA expression, indicating a direct inhibitory action on the pivotal mechanism of osteoclast formation (Bellido & Plotkin, 2011; Ruan et al., 2012). Finally, simvastatin can antagonize dexamethasone-induced osteoblastic apoptosis in a dose-dependent manner by increasing tissue levels of TGF-β, leading to activation of the SMAD3 metabolic pathway, which is essential for bone mass maintenance (Ruan et al., 2012; Oryan et al., 2015).

In the present study, the lowest doses of alendronate (G3, 0.2 mg/kg and G4, 0.4 mg/kg) were irrelevant to attenuate glucocorticoid-induced osteoporosis. In addition, the combination therapy has not always determined the best results compared with bisphosphonate monotherapy. It was clearly observed that animals receiving the highest dose of alendronate (G2, 0.8 mg/kg) showed similar or best morphological and biomechanical results compared with two groups treated with different combinations of sodium alendronate plus simvastatin (G6, 0.2 + 0.4 mg/kg and G7, 0.4 + 0.6, respectively). This finding corroborated previous evidences indicating that bisphosphonates and statins acts by an addictive mechanism rather than a synergic effect (Tanriverdi et al., 2005). As expected, appears to become coherent the proposition that the efficiency of both monotherapy and drugs combination is directly influenced by the dose administered. Therefore, finding optimal doses to develop effective drug combination represents an important challenge in the search for more rational schemes potentially applied in the therapeutic management of osteoporosis.

Conclusions

Taken together, our findings indicated that dexamethasone-induced osteoporosis in rats constitutes a robust model that shows the classical relationship between mechanical insufficiency and microstructural fragility of bone. In this model, reduced bone mechanical resistance was accompanied by marked depletion of collagenous and non-collagenous protein levels, bone mineral mass, pathological remodeling, and microstructural fragility of the cortical and cancellous bone. Although the administration of alendronate alone has not always been effective in attenuating all these morphofunctional bone damage and osteoporosis severity, the results of bisphosphonate therapy were enhanced when alendronate was combined with simvastatin, especially in the highest doses, showing a dose-dependent effect that was potentially related to the complementary mechanisms by which each drug induces bone anabolism, accelerating tissue repair in dexamethasone-induced osteoporosis.

Acknowledgments

This study was supported by the Brazilian agencies "Fundação de Amparo à Pesquisa do Estado de Minas Gerais – FAPEMIG" and "Conselho Nacional de Desenvolvimento Científico e Tecnológico – CNPq". The authors thank the "Núcleo de Microscopia and Micoanálise – NMM" of the Federal University of Viçosa by assistance in scanning electron microscopy.

Conflicts of Interest

The authors declare that they have no conflicts of interest.

References

Bellido, T. & Plotkin, L.I. (2011). Novel actions of bisphosphonates in bone: Preservation of osteoblast and osteocyte viability. *Bone* **49**, 50–55.

Bonucci, E. & Ballanti, P. (2014). Osteoporosis-bone remodeling and animal models. *Toxicol Pathol* **42**, 957–969.

Bouxsein, M.L., Boyd, S.K., Christiansen, B.A., Guldberg, R.E., Jepsen, K.J. & Müller, R. (2010). Guidelines for assessment of bone microstructure in rodents using micro-computed tomography. *J Bone Miner Res* **25**, 1468–1486.

Bradford, M. (1976). A rapid and sensitive method for quantitation of microgram quantities of protein utilizing the principle of protein-dye binding. *Anal Biochem* **72**, 248–254.

Briot, K. & Roux, C. (2015). Glucocorticoid-induced osteoporosis. *RMD Open* **1**, e000014.

Cruz-Orive, L., Karlsson, L., Larsen, S. & Wainschtein, F. (1992). Characterizing anisotropy: A new concept. *Micron Microsc Acta* **23**, 75–76.

Cupertino, M.C., Costa, K.L., Santos, D.C., Novaes, R.D., Condessa, S.S., Neves, A.C., Oliveira, J.A. & Matta, S.L. (2013). Long-lasting morphofunctional remodelling of liver parenchyma and stroma after a single exposure to low and moderate doses of cadmium in rats. *Int J Exp Pathol* **94**, 343–351.

Cupertino, M.D.C., Novaes, R.D., Santos, E.C., Bastos, D.S.S., Marques Dos Santos, D.C., do Carmo Queiroz Fialho, M. & Matta, S.L.P.D. (2017). Cadmium-induced testicular damage is associated with mineral imbalance, increased antioxidant enzymes activity and protein oxidation in rats. *Life Sci* **175**, 23–30.

Dai, L., Xu, M., Wu, H., Xue, L., Yuan, D., Wang, Y., Shen, Z., Zhao, H. & Hu, M. (2016). The functional mechanism of simvastatin in experimental osteoporosis. *J Bone Miner Metab* **34**, 23–32.

de Vries, F., Pouwels, S., Lammers, J.W., Leufkens, H.G., Bracke, M., Cooper, C. & van Staa, T.P. (2007). Use of inhaled and oral glucocorticoids, severity of inflammatory disease and risk of hip/femur fracture: a population-based case-control study. *J Intern Med* **261**, 170–177.

Dimic, A., Jankovic, D., Jankovic, I., Savic, T. & Karanovic, N. (2010). The effects of one-year simvastatin therapy on women's bone mineral density. *Cent Eur J Med* **6**, 98–102.

Garnero, P. (2008). Biomarkers for osteoporosis management: utility in diagnosis, fracture risk prediction and therapy monitoring. *Mol Diagn Ther* **12**, 157–170.

Gimble, J.M. & Nuttall, M.E. (2012). The relationship between adipose tissue and bone metabolism. *Clin Biochem* **45**, 874–879.

Grynpas, M.D., Tupy, J.H. & Sodek, J. (1994). The distribution of soluble, mineral-bound, and matrix-bound proteins in osteoporotic and normal bones. *Bone* **15**, 505–513.

Hlaing, T.T. & Compston, J.E. (2014). Biochemical markers of bone turnover – Uses and limitations. *Ann Clin Biochem* **51**, 189–202.

Hurson, C.J., Butler, J.S., Keating, D.T., Murray, D.W., Sadlier, D.M., O'Byrne, J.M. & Doran, P.P. (2007). Gene expression analysis in human osteoblasts exposed to dexamethasone identifies altered developmental pathways as putative drivers of osteoporosis. *BMC Musculoskelet Dis* **8**, 12.

Jia, D., O'Brien, C.A., Stewart, S.A., Manolagas, S.C. & Weinstein, R.S. (2006). Glucocorticoids act directly on osteoclasts to increase their life span and reduce bone density. *Endocrinology* **147**, 5592–5599.

Khosla, S., Bilezikian, J.P., Dempster, D.W., Lewiecki, E.M., Miller, P.D., Neer, R.M., Recker, R.R., Shane, E., Shoback, D. & Potts, J.T. (2012). Benefits and risks of bisphosphonate therapy for osteoporosis. *J Clin Endocrinol Metab* **97**, 2272–2282.

Kourkoumelis, N., Balatsoukas, I. & Tzaphlidou, M. (2012). Ca/P concentration ratio at different sites of normal and osteoporotic rabbit bones evaluated by Auger and energy dispersive X-ray spectroscopy. *J Biol Phys* **38**, 279–291.

Lucinda, L.M., Aarestrup, B.J., Peters, V.M., Reis, J.E., Oliveira, R.S. & Guerra, M.O. (2013). The effect of the Ginkgo biloba extract in the expression of Bax, Bcl-2 and bone mineral content of Wistar rats with glucocorticoid-induced osteoporosis. *Phytother Res* **27**, 515–520.

Mandarim-de-Lacerda, C.A. (2003). Stereological tools in biomedical research. *An Acad Bras Cienc* **75**, 469–486.

Manelli, F. & Giustina, A. (2000). Glucocorticoid-induced osteoporosis. *Trends Endocrinol Metab* **11**, 79–85.

Mclaughlin, F., Mackintosh, J., Hayes, B.P., McLaren, A., Uings, I.J., Salmon, P., Humphreys, J., Meldrum, E. & Farrow, S.N. (2002). Glucocorticoid-induced osteopenia in the mouse as assessed by histomorphometry, microcomputed tomography, and biochemical markers. *Bone* **30**, 924–930.

Miller, G.K., Valerio, M.G., Pino, M.V., Larson, J.L., Viau, A., Hamelin, N., Labbé, R. & Banks, C.M. (2000). Chronic effects of the novel glucocorticosteroid RPR 106541 administered to beagle dogs by inhalation. *Toxicol Pathol* **28**, 226–236.

Moraes, G.H.K., Rodrigues, A.C.P., Silva, F.A., Rostagno, H.S., Minafra, C.S. & Bigonha, S.M. (2010). Effects of dietary L-glutamic acid and K vitamin in the biochemical composition in femurs of broilers at 14 days of age. *Rev Bras Zootec* **39**, 796–800.

Nagashima, M., Takahashi, H., Shimane, K., Nagase, Y. & Wauke, K. (2012). Osteogenesis and osteoclast inhibition in rheumatoid arthritis patients treated with bisphosphonates alone or in combination with pitavastatin over an 18-month follow-up after more than 4 years of treatment with bisphosphonates. *Arthritis Res Ther* **14**, R224.

Nakashima, Y. & Haneji, T. (2013). Stimulation of osteoclast formation by RANKL requires interferon regulatory factor-4 and is inhibited by simvastatin in a mouse model of bone loss. *PLOS One* **8**, e72033.

Novaes, R.D., Penitente, A.R., Gonçalves, R.V., Talvani, A., Peluzio, M.C.G., Neves, C.A., Natali, A.J. & Maldonado, I.R.S.C. (2013). *Trypanosoma cruzi* infection induces morphological reorganization of the myocardium parenchyma and stroma, and modifies the mechanical properties of atrial and ventricular cardiomyocytes in rats. *Cardiovasc Pathol* **22**, 270–279.

Oryan, A., Kamali, A. & Moshiri, A. (2015). Potential mechanisms and applications of statins on osteogenesis: current modalities, conflicts and future directions. *J Control Release* **215**, 12–24.

Ribeiro, R.A., Ziegelmann, P.K., Duncan, B.B., Stella, S.F., da Costa Vieira, J.L., Restelatto, L.M., Moriguchi, E.H. & Polanczyk, C.A. (2013). Impact of statin dose on major cardiovascular events: A mixed treatment comparison meta-analysis involving more than 175,000 patients. *Int J Cardiol* **166**, 431–439.

Rogers, M.J., Crockett, J.C., Coxon, F.P. & Mönkkönen, J. (2011). Biochemical and molecular mechanisms of action of bisphosphonates. *Bone* **49**, 34–41.

Rosenson, R.S., Tangney, C.C., Langman, C.B., Parker, T.S., Levine, D.M. & Gordon, B.R. (2005). Short-term reduction in bone markers with high-dose simvastatin. *Osteoporos Int* **16**, 1272–1276.

Ruan, F., Zheng, Q. & Wang, J. (2012). Mechanisms of bone anabolism regulated by statins. *Biosci Rep* **32**, 511–519.

Russell, R.G.G. (2011). Bisphosphonates: The first 40 years. *Bone* **49**, 2–19.

Sasaki, N., Kusano, E., Ando, Y., Yano, K., Tsuda, E. & Asano, Y. (2001). Glucocorticoid decreases circulating osteoprotegerin (OPG): Possible mechanism for glucocorticoid induced osteoporosis. *Nephrol Dial Transplant* **16**, 479–482.

Sequetto, P.L., Oliveira, T.T., Maldonado, I.R., Augusto, L.E., Mello, V.J., Pizziolo, V.R., Almeida, M.R., Silva, M.E. & Novaes, R.D. (2014). Naringin accelerates the regression of pre-neoplastic lesions and the colorectal structural reorganization in a murine model of chemical carcinogenesis. *Food Chem Toxicol* **64**, 200–209.

Sequetto, P.L., Oliveira, T.T., Soares, I.A., Maldonado, I.R., Mello, V.J., Pizziolo, V.R., Almeida, M.R. & Novaes, R.D. (2013). The flavonoid chrysin attenuates colorectal pathological remodeling reducing the number and severity of pre-neoplastic lesions in rats exposed to the carcinogen 1,2-dimethylhydrazine. *Cell Tissue Res* **352**, 327–339.

Shefrin, A.E. & Goldman, R.D. (2009). Use of dexamethasone and prednisone in acute asthma exacerbations in pediatric patients. *Can Fam Physician* **55**, 704–706.

Soares, E.A., Novaes, R.D., Nakagaki, W.R., Fernandes, G.J., Garcia, J.A. & Camilli, J.Á. (2015). Metabolic and structural bone disturbances induced by hyperlipidic diet in mice treated with simvastatin. *Int J Exp Pathol* **96**, 261–268.

Sunyecz, J. (2008). Optimizing dosing frequencies for bisphosphonates in the management of postmenopausal osteoporosis: patient considerations. *Clin Interv Aging* **3**, 611–627.

Tanriverdi, H.A., Barut, A. & Sarikaya, S. (2005). Statins have additive effects to vertebral bone mineral density in combination with risedronate in hypercholesterolemic postmenopausal women. *Eur J Obstet Gynecol Reprod Biol* **120**, 63–68.

Tsubaki, M., Satou, T., Itoh, T., Imano, M., Yanae, M., Kato, C., Takagoshi, R., Komai, M. & Nishida, S. (2012). Bisphosphonate- and statin-induced enhancement of OPG expression and inhibition of CD9, M-CSF, and RANKL expressions via inhibition of the Ras/MEK/ERK pathway and activation of p38MAPK in mouse bone marrow stromal cell line ST2. *Mol Cell Endocrinol* **361**, 219–231.

Vasikaran, S., Eastell, R., Bruyère, O., Foldes, A.J., Garnero, P., Griesmacher, A., McClung, M., Morris, H.A., Silverman, S., Trenti, T., Wahl, D.A., Cooper, C. & Kanis, J.A., IOF-IFCC Bone Marker Standards Working Group (2011). Markers of bone turnover for the prediction of fracture risk and monitoring of osteoporosis treatment: A need for international reference standards. *Osteoporos Int* **22**, 391–420.

Weiner, S. & Wagner, H.D. (1998). The material bone: Structure mechanical function relations. *Annu Rev Mater Sci* **28**, 271–298.

Weinstein, R.S. (2001). Glucocorticoid-induced osteoporosis. *Rev Endocr Metab Disord* **2**, 65–73.

Weinstein, R.S. (2012). Glucocorticoid-induced osteoporosis and osteonecrosis. *Endocrinol Metab Clin North Am* **41**, 595–611.

Wheater, G., Elshahaly, M., Tuck, S.P., Datta, H.K. & van Laar, J.M. (2013). The clinical utility of bone marker measurements in osteoporosis. *J Transl Med* **11**, 201.

Whittier, X. & Saag, K. (2016). Glucocorticoid-induced osteoporosis. *Rheum Dis Clin North Am* **42**, 177–189.

Xu, X.C., Chen, H., Zhang, X., Zhai, Z.J., Liu, X.Q., Qin, A. & Lu, E.Y. (2014). Simvastatin prevents alveolar bone loss in an experimental rat model of periodontitis after ovariectomy. *J Transl Med* **12**, 284.

Zhang, Y., Bradley, A.D., Wang, D. & Reinhardt, R.A. (2014). Statins, bone metabolism and treatment of bone catabolic diseases. *Pharmacol Res* **88**, 53–61.

Zimmermann, E.A., Busse, B. & Ritchie, R.O. (2015). The fracture mechanics of human bone: Influence of disease and treatment. *Bonekey Rep* **4**, 743.